In Vitro Cell.Dev.Biol.—Animal (2016) 52:107–119
DOI 10.1007/s11626-015-9950-7

Effect of sesamin against cytokine production from influenza type A H1N1-induced peripheral blood mononuclear cells: computational and experimental studies

Kanda Fanhchaksai[1] · **Kanchanok Kodchakorn**[1,2] · **Peraphan Pothacharoen**[1] · **Prachya Kongtawelert**[1]

Received: 27 May 2015 / Accepted: 18 August 2015 / Published online: 30 September 2015 / Editor: Tetsuji Okamoto

Abstract In 2009, swine flu (H1N1) had spread significantly to levels that threatened pandemic influenza. There have been many treatments that have arisen for patients since the WHO first reported the disease. Although some progress in controlling influenza has taken place during the last few years, the disease is not yet under control. The development of new and less expensive anti-influenza drugs is still needed. Here, we show that sesamin from the seeds of the Thai medicinal plant *Sesamum indicum* has anti-inflammatory cytokines in human peripheral blood mononuclear cells (PBMCs) induced by 2009 influenza virus type A H1N1. In this study, the combinatorial screening method combined with the computational approach was applied to investigate the new molecular binding structures of sesamin against the 2009 influenza virus type A H1N1 (p09N1) crystallized structure. Experimental methods were applied to propose the mechanisms of sesamin against cytokine production from H1N1-induced human PBMC model. The molecular dynamics simulation of sesamin binding with the p09N1 crystallized structure showed new molecular binding structures at ARG118, ILE222, ARG224, and TYR406, and it has been proposed that sesamin could potentially be used to produce anti-H1N1 compounds. Furthermore, the mechanisms of sesamin against cytokine production from influenza type A H1N1-induced PBMCs by ELISA and signaling transduction showed that sesamin exhibits the ability to inhibit proinflammatory cytokines, IL-1β and TNF-α, and to enhance the activity of the immune cell cytokine IL-2 via downregulating the phosphorylated JNK, p38, and ERK1/2 MAPK signaling pathways. This information might very well be useful in the prevention and treatment of immune-induced inflammatory disorders.

Keywords Influenza type A H1N1 virus · Sesamin · Peripheral blood mononuclear cells · Influenza A neuraminidase · Molecular dynamics simulation

Kanda Fanhchaksai and Kanchanok Kodchakorn contributed equally to this work.

Electronic supplementary material The online version of this article (doi:10.1007/s11626-015-9950-7) contains supplementary material, which is available to authorized users.

✉ Prachya Kongtawelert
prachya.kongtawelert@gmail.com

Kanda Fanhchaksai
iamkanda54@gmail.com

Kanchanok Kodchakorn
tkanchanok@gmail.com

Peraphan Pothacharoen
peraphan.pothacharoen@gmail.com

[1] Thailand Excellence Center for Tissue Engineering and Stem Cells, Department of Biochemistry, Faculty of Medicine, Chiang Mai University, Chiang Mai 50200, Thailand

[2] Computational Simulation and Molecular Modeling Laboratory (CSML), Department of Chemistry, Faculty of Science, Chiang Mai University, Chiang Mai 50200, Thailand

Introduction

After the first reported case in March 2009, the 2009 H1N1 influenza virus traveled beyond borders and even across continents (Dawood *et al.* 2009). Canadian health authorities demonstrated that the transmission occurred only on a human-to-human basis, and noted that this widespread virus was different from the virus of the swine flu that is common among pigs. Thus, the mechanical pathway in the case of the actual H1N1 2009 influenza is very complicated to fully comprehend (Chambers *et al.* 1991) and has also retained a

significant health problem (Dai *et al.* 2011). Type A influenza belongs to the "Orthomyxoviridae family," a family of RNA viruses that includes five genera: influenza virus A, influenza virus B, influenza virus C, isavirus, and thogotovirus. These are common viruses that are found among humans, birds, pigs, as well as many other mammals (Büchen-Osmond 2006). The symptoms of this type of influenza include respiratory problems such as coughing and sneezing and high fever. However, in cases of strong infection and a weak immune system, the effects may be more severe, causing deadly symptoms such as pneumonia.

The influenza A virus is a single-stranded RNA virus with a viral envelope and a segmented genome (Committee WHOE 1980). The virus attaches to the host's sialylated glycoproteins via the viral hemagglutinin (HA) and enters the cell by endocytosis. The viral genomic ribonucleoprotein (RNP) translocates to the nucleus where transcription and replication of viral RNA occurs. During the infection of the influenza virus, specific host receptors can recognize the viral proteins, such as HA, neuraminidase (NA), and M2 proteins that are essential for viral particle formation and budding from host cells via the secretory pathway (Palese *et al.* 2007), which initiates a series of signal transductions of innate immune response to the virus infection known as "cytokine storm" (Mogensen *et al.* 2001).

At present, natural products derived from plants are being investigated for their therapeutic benefits due to the increased popularity of local medicinal plants used in the treatment of many types of diseases. Many of these plants show antimicrobial activity (Cowan 1999). Sesame is a Thai herb that is widely consumed in Thailand and is found in *Sesamum indicum* seeds, which contain two unique lignan substances, sesamin and sesamolin. To date, there have been many research reports that have studied the biological activity of sesamin. The work of Wang *et al.* (2002) has clearly demonstrated that sesamin reduces lipopolysaccharide (LPS)-induced nitric oxide (NO) production in macrophages, which are induced by nuclear transcription factors. Moreover, sesamin has been shown to decrease matrix metalloprotease expression, which can degrade both proteoglycans and type II collagen, resulting in a release of sulfated glycosaminoglycan and hydroxyproline induced by IL-1β in porcine cartilage explants (Phitak *et al.* 2012).

In this study, a computational approach was applied to investigate the new molecular binding structures of sesamin that can successfully inhibit the 2009 influenza virus type A H1N1. In addition, sesamin was used to investigate the effect of anti-inflammatory cytokine using influenza type A H1N1-induced human peripheral blood mononuclear cells (PBMCs) as models. It was found that sesamin could reduce neuraminidase activity and inhibit the cytokine storm in the reduction of the IL-1β and TNF-α release. This is possible due to its properties, which can enhance the activity of immune cells of IL-2 along with its protein release while at the same time downregulating the phosphorylated c-Jun N-terminal kinase (JNK), p38, and ERK1/2 mitogen-activated protein kinase (MAPK) signaling pathways. These findings may in fact lead to the development of new antiviral drugs from natural product compounds.

Materials and Methods

Materials. The purified sesamin was obtained from Assoc. Prof. Dr. Wilart Pompimon, Lampang Province of Thailand, and the voucher specimen (BKF no. 138181) has been deposited at the Forest Herbarium, Royal Forestry Department, Ministry of Natural Resource and Environment, Bangkok, Thailand. The powdered seeds of *S. indicum* Linn were extracted and separated by column chromatography over silica gel (Merck No. 7734, mesh 70–230 ASTM). The separated sesamin was crystallized with ethanol to yield colorless needle crystals and was identified by MS/NMR. The sesamin was characterized using the HPLC method and compared to standard sesamin (Sigma-Aldrich®, St. Louis, MO).

Computational methods. The initial structure of the 2009 pH1N1 N1 NA (p09N1) complex was taken from the X-ray crystallography structure with the PDB code of 3TI6 (Vavricka *et al.* 2011). The amino acid sequences of p09N1 and the ligand structures in each complex are shown in Figs. S1 and 1, respectively. The 3D structures of the Thai medicinal plant sesamin were built and optimized (1000 steps of the adopted basis Newton-Raphson—ABNR) using the CHARMm force field in the Discovery Studio (DS) 2.5 package (Accelrys Software Inc., San Diego, CA). The structures of proteins and inhibitors were utilized in subsequent docking experiments with CDOCKER protocols (Wu *et al.* 2003) in the DS 2.5 package. The energy minimization and molecular dynamics (MD) simulations were performed using PMEMD.CUDA from AMBER12 (Case *et al.* 2005) on GPUs Geforce GTX780 produced by NVIDIA, which sped up the simulation wall time that is required to obtain the trajectory files from each simulation. All MD systems were simulated under the same conditions, and all experiments were performed under periodic boundary conditions (Weber *et al.* 2000). Each of the complexes' structure was solvated in a cubic box of TIP3P water extending to at least 12 Å in each direction from the solute, and the cutoff distance was kept to 15 Å in order to compute the nonbonded interactions and Na^+ ions as the neutralizing countering ions. The AMBER ff12SB force field parameters were applied in order to describe the molecular characteristics of the complexes. The long-range electrostatics were treated using the particle mesh Ewald (PME) method (Darden *et al.* 1993). The SHAKE algorithm and the Langevin dynamics were applied to constrain the bonds involving hydrogen and to control the temperature.

The time step was set to 2 fs and the trajectory was recorded every 0.2 ps. First, all docked complexes were energy-minimized to remove any bad contacts and to achieve a good starting structure, which would enable the performance of the molecular dynamics simulations. The first step was to allow, out of 10,000 iterations, only water molecules to move. In the second step, each of the 10,000 iterations, hydrogen and protein side chains were relaxed, in a fixed order. Finally, 20,000 iterations were calculated with the restriction-free system. After that, the MD simulations were performed according to the following steps: initially, the temperature of each system was increased by gradually heating the NVT (constant number of atoms, volume, and temperature) dynamics with the fixed protein atoms over 60 ps from 0 to 310.15 K. This was done by using a force constant of 10 kcal mol^{-1} $Å^{-2}$. Then, the first 200-ps pressure-constant periods (NPT; constant number of atoms, pressure, and temperature) were applied to obtain the equilibrated density of the constrained protein atoms at a force constant of 5.0 kcal mol^{-1} $Å^{-2}$. Next, the second group of 200 ps dynamics at no force was applied to the protein atoms. Finally, 20 ns of unrestrained NPT-MD simulations (no force applied to any protein atoms) were performed for each fully flexible system at 310.15 K and 1 atm. The density of each system was about 1.0 g/cm^3. At the end of the equilibration period, all memory of the initial configuration was intentionally lost. This was done so that the final results would not depend on the initial configuration. Following the equilibration period, the structural properties and intermolecular interactions of each MD system were analyzed based on the MD trajectories from the last 10 ns. Binding free energy calculations were based on selected MD snapshots, and the energy components were calculated using a very large cutoff (999 Å). The molecular mechanics Poisson-Boltzmann surface area (MM-PBSA) (Donini *et al.* 2000) and the molecular mechanics generalized Born surface area (MM-GBSA) (Chong *et al.* 1999) protocols were applied in order to calculate the binding free energy of each complex system. In this study, the binding free energy of each system was calculated from 11–15 to 15–20 ns of the trajectories. The 2500 snapshots were extracted from each range, and the grid size for the PB calculations in MM-PBSA was 0.5 Å. The enzyme-ligand interaction energy profiles were generated by decomposing the total binding free energies into residue-residue interaction pairs via the MM-GBSA decomposition process in the mm_pbsa program of AMBER12 (Gohlke *et al.* 2003; Hou *et al.* 2008). The values of the interior and exterior dielectric constants in MM-GBSA were set to 1 and 80, respectively. The exploration of the hot spots on p09N1 and oseltamivir or sesamin was discussed, as well was an assessment of the amino acid residues' effects on the binding affinity of each complex in aqueous solution.

Assay of neuraminidase inhibition activity. The assay is based on the measurement of total sialic acid (TSA) released from bovine submaxillary mucin (Kongtawelert *et al.* 2003). Briefly, 50 μl of each sample, oseltamivir and sesamin, was incubated with or without neuraminidase enzymes at 37°C for 60 min. After that, these samples were incubated with mucin as the substrate or standard sialic acid (2–10 μg/well) for 15 min. The solutions were added to a 96-well plate. Then, 50 μl of 1.3 mM periodic acid was added to each well and they were mixed for 5 min. After being incubated in an icebox for 60 min, 100 μl of 0.6% (*w*/*w*) of resorcinol reagent was added and the solutions were mixed for 5 min. The plate was heated to 80°C for 60 min in a bath of hot water and then shaken with a shaker for 2 min. The plate's contents were cooled to room temperature. Finally, 100 μl of 95% *t*-butyl alcohol was added and mixed for 5 min before being immediately measured at 620 nm using a microplate reader spectrophotometer. The values were converted to neuraminidase activity (units/ml) using a standard curve.

PBMC preparation and culture. PBMCs were isolated from whole blood samples using the density-gradient centrifugation technique (Brincks *et al.* 2008). The whole blood samples were heparinized and diluted with sterile PBS at a ratio of 1:1. They were under-layered with Ficoll-Hypaque (Sigma-Aldrich®) and centrifuged at 400×*g* for 30 min. The PBMC layer was collected and washed with sterile PBS. The PBMCs were cultured in RPMI 1640 medium (Gibco, Grand Island, NY) that was supplemented with penicillin/streptomycin (100 U/100 μg/ml) and gentamicin 40 mg/ml at 37°C in a humidified incubator containing 5% CO_2. The cytotoxicity of sesamin and oseltamivir (Tamiflu®) in the PBMCs was investigated using the Alamar Blue solution as described in the Supplementary Data section.

Influenza type A H1N1 preparation and culture. The influenza virus type A H1N1, inactivated by β-propiolactone (Garlick *et al.* 1976; Honda-Okubo *et al.* 2014), was obtained from Prof. Yong Poovorawan, Faculty of Medicine, Chulalongkorn University, Bangkok, Thailand. The inactivated influenza virus type A H1N1 at a titer of 128 hemagglutination units (HAU), which is a protein-based virus quantification assay, and embryonated chicken eggs that had been propagated with the virus were used in the control group.

For H1N1-induced PBMCs and treatments, PBMCs (8×10^5 cells/ml) were plated in a 24-well plate and induced with or without H1N1. Cells were cotreated with different concentrations of sesamin (or oseltamivir) and incubated at 37°C with 5% CO_2 for 24 h, which was a modified method based on the work of Brincks et al. (2008). After 24 h of treatment, the media were collected for the purposes of measuring human IL-1β, TNF-α, and IL-2 proteins using the enzyme-linked immunosorbent assay (ELISA), and the cells were collected for the purposes of measuring cytokine messenger RNA

(mRNA) levels using real-time reverse transcription polymerase chain reaction (RT-PCR).

Measurement of cytokines. After 24 h of treatment, the levels of cytokine released to the media were determined using the human IL-1β, TNF-α, and IL-2 Biotrak Easy ELISA kit according to the manufacturer's instructions (Amersham, GE Healthcare, Buckinghamshire, UK). Briefly, 150 μl of standard diluent buffer and 100 μl of deionized water were added to each well of an eight-well strip plate coated with human polyclonal IL-1β or TNF-α or IL-2 antibodies. Then, 50 μl of each sample with sesamin or oseltamivir (0.5, 1.0, and 5.0 μg/ml) was added and incubated for 3 h at room temperature. After incubation, these standards and samples were washed with washing buffer (400 μl/well) four times. Then, 100 μl of premixed TMB substrate was added to each well and they were then incubated at room temperature for 15 min in the dark, and then 100 μl of the stop solution was added. The optical density was measured at 450 nm using the Titertek Multiskan M340 multiplate reader, and the values were converted to concentrations using a standard curve. The cytokines released from the culture medium of influenza type A H1N1-induced PBMCs were estimated using the following calculation:

$$\%\text{cytokine relative} = \left[\frac{\text{sample medium}}{\text{embryonated chicken egg}}\right] \times 100$$

Gene expression analysis. Total RNA from sesamin or oseltamivir cotreated with H1N1- induced PBMCs was extracted using Nucleospin™ RNA II procedure (Macherey-Nagel, Düren, Germany) according to the manufacturer's instructions. Total RNA (500 ng) of each sample was used to reverse for complementary DNA (cDNA) synthesis using RevertAid™ First Strand cDNA synthesis kit (MBI Fermentas, St. Leon-Rot, Germany). Real-time RT-PCR was performed in a DNA Engine (ABi 7500) using SYBR® GreenER™ qPCR SuperMix Universal (Invitrogen, Waltham, MA). The program used for amplification was as follows: 95°C for 10 min, then 55 cycles of denaturation at 95°C for 15 s, annealing at 60°C for 15 s, and elongation at 72°C for 33 s. The sequence primers of cytokine markers IL-1β (Boeuf *et al.* 2005), TNF-α (Boeuf *et al.* 2005), and IL-2 (Provenzano *et al.* 2003) are shown in Table S1. Relative expression levels for each primer set were normalized to the expression of GAPDH by the $2^{-\Delta\Delta C}{}_{T}$ method (Livak *et al.* 2001).

Western blotting analysis. H1N1-induced PBMCs that were treated with sesamin from 0.5 to 5.0 μg/ml for 1 h were lysed with a 2× sample buffer containing 5% β-mercaptoethanol. Samples were subjected to 10% SDS-PAGE under a reducing condition. The proteins were electrotransferred to the polyvinylidene difluoride membrane, and the membrane was soaked in 5% skim milk in TBS containing 0.1% Tween-20 (TBS-T) for blocking. The membrane was probed with rabbit anti-phosphorylated p44/42 MAPK, rabbit anti-phosphorylated p38, rabbit anti-phosphorylated SPAK/JNK, rabbit anti-p44/42 MAPK, rabbit anti-p38, and rabbit anti-SPAK/JNK antibodies (Cell Signaling Technology®, Danvers, MA) at 4°C overnight. The primary antibodies (diluted 1:1000) and secondary antibodies consisting of horseradish peroxidase-labeled anti-rabbit antibodies (diluted 1:2000) were used for the detection procedure. After washing the membrane three times with TBS-T, a signal was detected with the ECL detection system (KPL® system). The immune-positive bands were visualized using the Chemi XRS Gel Documentation System (Bio-Rad, Berkeley, CA). The relative intensities of the immune-positive bands were calculated using Quantity One 4.6.5 software and compared to those measured in the embryonated chicken eggs of the control group. The comparison was made using the following calculation:

$$\text{MAPK signaling ratio} = \frac{\left[\frac{\text{phosphorylated form of the sample}}{\text{total form of the sample}}\right]}{\left[\frac{\text{phosphorylated form of the control}}{\text{total form of the control}}\right]}$$

Statistical analysis. All data was expressed in terms of the mean and standard error (mean±SE) of the independent triplicate samples. Differences were analyzed by Student's *t* test. Any *p* value found to be less than 0.05 was considered significant.

Results

Sesamin possessing hot spot amino acids in a binding region of the 2009 influenza virus type A H1N1: computational modeling method. An investigation of the possibility of sesamin binding on the targeted protein in the 2009 influenza virus type A H1N1 (p09N1) was done using the computational method. The initial structure of the p09N1 complex was taken from the X-ray crystallography structure with PDB code of 3TI6 (Vavricka *et al.* 2011). The amino acid sequences of p09N1 are shown in Fig. S1. The 2D structure of sesamin was built (Fig. 1) and docked with the p09N1 using the CDOCKER protocol (Wu *et al.* 2003) as implemented in the DS 2.5 program (Accelrys Software Inc.), according to the above docking protocol. The interaction energies of the complex structures were calculated with the CDOCKER protocol.

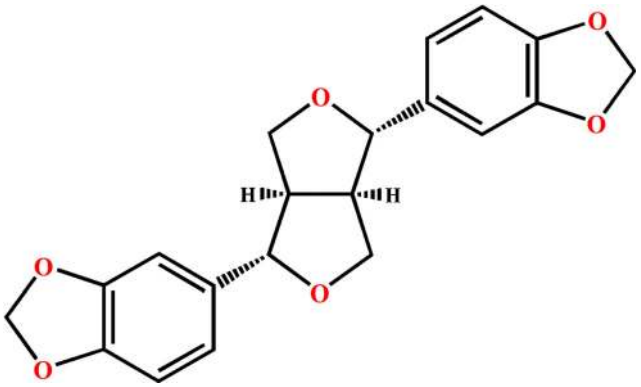

Figure 1. The two-dimensional (2D) structure of sesamin.

Moreover, the docked conformations revealed that sesamin was located in the hydrophobic/hydrophilic binding region; however, the side chains of the amino acids in the binding pockets were kept flexible during the docking simulation. The scoring functions in Table 1 suggest that the interactions of the optimum docking structures reflect the negative binding energies, indicating that sesamin has a favorable binding with p09N1 when compared to that of oseltamivir and zanamivir, which were used as positive models. Moreover, the residues in the binding pockets of p09N1 consisted of different combinations of nonpolar, polar, acidic, and basic moieties. In the binding pockets, the complementary hydrophobic and hydrophilic interactions of the common amino acids in p09N1 were observed, which facilitate the protein-ligand binding within 3 Å of oseltamivir, and these are ARG118, GLU119, ASP151, ARG152, TRP178, ARG224, SER246, GLU276, GLU277, ARG292, ASN294, ARG371, and TYR406. The same interactions are seen when using zanamivir. However, the binding pockets within 3 Å of sesamin show the interaction of different amino acids. These are ARG118, GLU119, PRO120, ARG152, ARG156, TYR406, TRP423, GLU425, ILE427, PRO431, and LYS432 as shown in Table 1.

To confirm the geometry configuration properties and conformational changes, the p09N1 complexes with oseltamivir, zanamivir, and sesamin were calculated based on the root-mean-squared deviations (RMSD) of all C_α-atoms (Fig. 2) by a MD simulation. The simulation observations and results showed that most of the complexes fluctuated within the small range of 1.0 to 1.5 Å. In contrast, both RMSD of p09N1-sesamin and p09N1-oseltamivir remained at steady levels between 1 and 9 ns, but afterward, p09N1-oseltamivir fluctuated between 1.2 and 1.7 Å. The results showed that p09N1-sesamin and p09N1-oseltamivir (and zanamivir) did not differ much in terms of the geometric configuration structures and their structural stability. Also, it is of importance to note that the position of sesamin remained fairly constant with minimal deviation within the binding pockets. Therefore, each of the docked ligands had a different amount of structural stability in the complexes during the MD simulations. The Ligplot analyses were used to understand the hot spots' interaction pattern, especially those of the hydrophobic interactions as well as the hydrogen bonding pattern between the simulated ligands and the p09N1 active site residues (Wallace *et al.* 1995). Figure 3 shows the 2D Ligplot diagrams from the MD simulation for the three compounds which were previously discussed in the section on docking simulations. For p09N1-sesamin, the essential amino acid ARG118 is only shown with H-bond interactions in Table 1 of the docking results, which were obtained for all of the compounds. These results prove that the p09N1-docked energy had the lowest binding energy levels with sesamin (−38.1 kcal mol^{-1}) when compared to the energy levels with oseltamivir (−83.2 kcal mol^{-1}) and zanamivir (−64.1 kcal mol^{-1}). However, from the MD simulation results, the capability of the p09N1-sesamin complex was observed to form hydrophobic interactions consisting of hot key residues of GLU119 and TYR406 along with GLU227, TRP423, GLU425, and LYS432. Hence, Ligplot analyses were especially useful in proving the hot spots' hydrophobic interaction pattern.

For use in future studies, it should be clarified that the binding interaction in the binding regions was calculated using the MM-PBSA methodology in order to gather data on the binding free energies (PB_{TOT}; kcal mol^{-1}) of all of those complexes. Table 2 lists the values of PB_{TOT} that were used

Table 1. PMF scores and amino acid residues in the binding region at 3 Å

Name	Binding energy (kcal mol^{-1})	Key amino acid in 3 Å from ligands	
		Nonpolar hydrophobic	Polar hydrophilic
Oseltamivir	−83.2	TRP178	**ARG118, GLU119**, ASP151, **ARG152**, ARG224, GLU276, ARG292, ASN294, ARG371, **TYR406**
Zanamivir	−64.1	LEU134, TRP178, ILE223	**ARG118, GLU119**, ASP151, **ARG152**, ARG156, GLU227, GLU276, GLU277, ARG292, ASN294, ARG371, **TYR406**
Sesamin	−38.1	TRP423, ILE427	**ARG118, GLU119**, PRO120, **ARG152**, ARG156, GLU227, **TYR406**, GLU425, PRO431, LYS432

The key amino acids are in *boldface type*

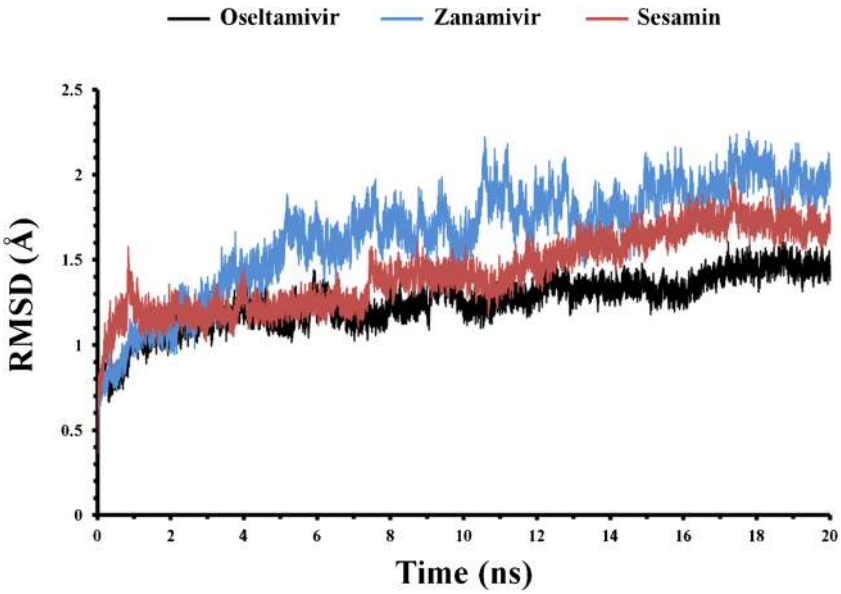

Figure 2. Root-mean-squared deviations (RMSD) of all C_α-atoms of the p09N1 complexes with oseltamivir (*black*), zanamivir (*blue*), and sesamin (*red*) as functions of simulation time.

for comparison between the simulation complexes. The values shown in Table 2 reveal more negative values, indicating more favorable conditions for binding. The calculations from MM-PBSA between 1 and 20 ns corresponded with the MM-GBSA protocol. The binding energies that were identified by the MM-PBSA protocol between 11 and 20 ns are listed as follows: oseltamivir>zanamivir>sesamin, with values of −29.18, −27.20, and −15.10 kcal mol^{-1}, respectively. The major contributions to the binding free energy arose from electrostatic energy as calculated by the molecular mechanic (MM) force field (ELE) from the electrostatic contribution to the solvation free energy as calculated by PB (PB_{CAL}) and from the van der Waals contribution from MM (VDW). Concerning the first two binding ligands, both VDW and ELE showed calculations that varied between low- and high-activity groups. These calculations indicate that both terms are factors that determine the binding activity. Sesamin did have a lower electrostatic contribution (−4.5 kcal mol^{-1}). The result does not equal the real binding free energy levels since the entropy contribution to the binding was not estimated in this study. However, the results suggest that the structural properties of sesamin, which is a hydrophilic, may play a role—however poorly—in the binding affinity in differently pocked regions in the binding sites.

Finally, to verify the hot key residue interactions, the MM-GBSA protocol was used to calculate the binding free energy of the docked complexes. This was done using the parameterization of Tsui and Case (Sali *et al.* 1993). Thus, the most important residues showed the more negative contributions, which are the strongest interactions of docked ligands in the binding pockets. Figure 4 shows a plot of the decomposed energies (kcal mol^{-1}) versus the significant amino acid

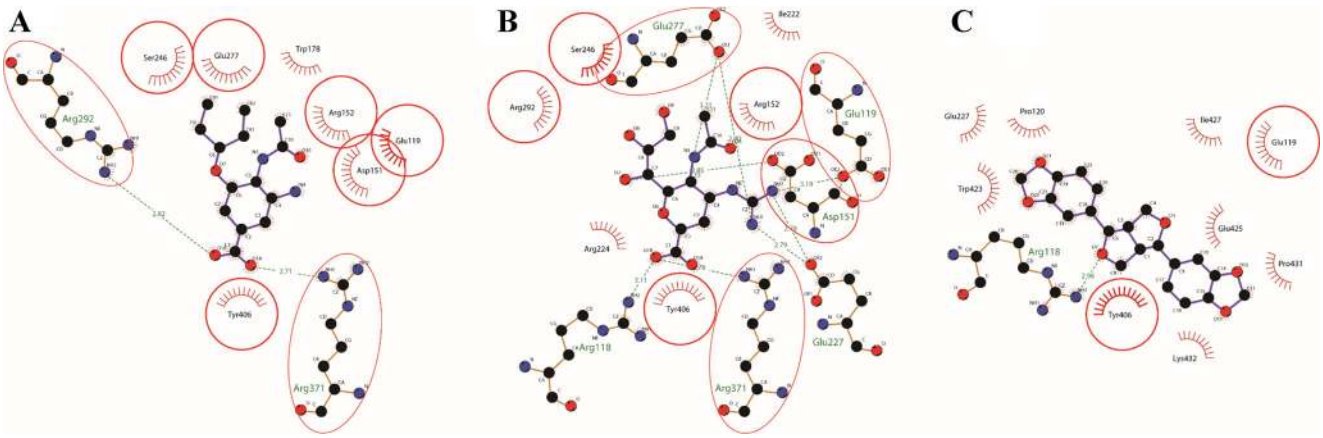

Figure 3. The 2D Ligplot diagram representations of ligand-protein interactions were analyzed between the p09N1 binding sites and (*A*) oseltamivir, (*B*) zanamivir, and (*C*) sesamin. The *red circles* and *ellipses* in each plot indicate protein residues that are in equivalent 3D positions to the residues in the first plot. Hydrogen bonds are shown as *green dotted lines*, and residues interacting through hydrophobic interactions are represented as spoked arcs in *red*.

Table 2. Binding free energies (kcal mol^{-1}) resulting from MM-PBSA/GBSA calculation of the p09N1 complexes with oseltamivir, zanamivir, and sesamin during 1–10 and 11–20 ns of the MD simulations

Method	Contribution	Energy in each contribution (kcal mol^{-1})					
		p09N1-oseltamivir		p09N1-zanamivir		p09N1-sesamin	
		1–10 ns	11–20 ns	1–10 ns	11–20 ns	1–10 ns	11–20 ns
MM	ELE	−195.5	−196.0	−183.2	−156.1	−9.2	−4.5
	VDW	−29.5	−26.9	−31.5	−30.0	−39.5	−34.6
	INT	0.0	0.0	0.0	0.0	0.0	0.0
	GAS	−224.9	−222.9	−214.8	−186.1	−48.7	−39.1
PBSA	PB_{SUR}	−5.2	−5.2	−5.1	−4.9	−5.6	−4.9
	PB_{CAL}	202.8	198.8	183.7	163.8	42.4	28.9
	PB_{SOL}	197.7	193.7	178.7	158.9	36.9	24.0
	PB_{ELE}	7.4	2.8	0.5	7.8	33.3	24.4
	PB_{TOT}	−27.3	*−29.2*	−36.1	*−27.2*	−11.8	*−15.1*
GBSA	GB_{SUR}	−5.1	−5.1	−5.1	−4.9	−5.5	−4.7
	GB_{CAL}	178.3	177.9	168.4	148.1	23.1	15.3
	GB_{SOL}	173.2	172.8	163.4	143.3	17.6	10.5
	GB_{ELE}	−17.2	−18.2	−14.8	−7.9	13.9	10.8
	GB_{TOT}	−51.8	*−50.1*	−51.4	*−42.9*	−31.1	*−28.6*

The significantly values in intalics are refered to the total binding free energy calculated by the MMPBSA or MM-GBSA methods

ELE accounts for the electrostatic interactions, VDW denotes the van der Waals interactions between the fragments, GAS accounts for the addition ELE+VDW+INT being the binding enthalpic contributions in vacuo, PB_{SUR} accounts for the nonpolar contribution to solvation, PB_{CAL} is the polar contribution of solvation, PB_{SOL} denotes the PB_{SUR}+PB_{CAL}, PB_{ELE} accounts for the PB_{CAL}+ELE addition, and PB_{TOT} accounts for the total binding free energy calculated by the MM-PBSA method

residues in the binding pockets of p09N1 for each of the docked ligands. All amino acids in the p09N1 sequence were found to exhibit positive or negative influences on the bindings with substrate molecules. Several residues of oseltamivir were verified to have significant and effective contributions to the absolute relative energy that was larger than 1 kcal mol^{-1} for the stabilization energy. The p09N1 is classified into group 1 serotype, based upon its primary sequence (Colman 1994; Russell *et al.* 2006), which comprised a 150-cavity formation (amino acids 147–151) of amino acids in the active sites. Group 2 does not have this in its sequence (Vavricka *et al.* 2011). Additionally, the 430-loop in those active sites plays a critical confederacy role with the 150-loop for the 150-cavity formation. The MD simulations also illustrated some

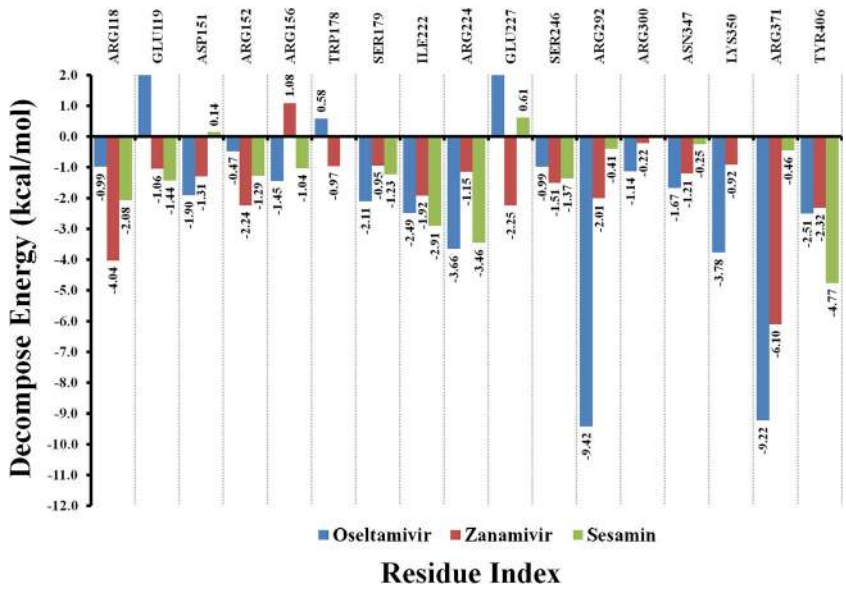

Figure 4. Decomposed energies (kcal mol^{-1}) of the amino acid residues of p09N1 with oseltamivir (*blue*), zanamivir (*red*), and sesamin (*green*) during 11–20 ns simulations.

differences in the flexibility of the 150-loop between oseltamivir and sesamin. Recent configuration studies reveal that ASP151 and ARG152 of the 150-loop form a hot spot key amino acid that interacts with oseltamivir at the 4-group and N-acetyl group, respectively. The results showed that there were four amino acid residues: ARG118 (−2.08), ILE222 (−2.91), ARG224 (−3.46), and TYR406 (−4.77). All of these showed strong negative (kcal mol^{-1}) bindings with sesamin at levels which correlated with those of the binding amino acid residues with both oseltamivir and zanamivir. In addition, the residues which showed strong negative bindings with oseltamivir were ASP151 (−1.90), SER179 (−2.11), ILE222 (−2.49), ARG224 (−3.66), ARG292 (−9.42), LYS350 (−3.78), ARG371 (−9.22), and TYR406 (−2.51). The residue bindings with zanamivir exhibited the strongest binding levels with different amino acids such as ARG118 (−4.04), ARG152 (−2.24), GLU227 (−2.25), and ARG371 (−6.10). The 150-loop formed hot spot key amino acid interactions that showed differences in each case between ASP151 and oseltamivir (−1.90), as well as with sesamin (0.14). The interactions between ARG152 with zanamivir (−2.24) and with sesamin (−1.29) were also observed. Also, PRO431 showed a more favorable binding interaction with sesamin (−4.04) than with oseltamivir (0.01). These interactions made a significant contribution to the overall binding for the stabilization of the structures during the MD simulations. The simulation results suggested that the hot spots' interactions consist of residues of ARG118, ILE222, ARG224, and TYR406, whereas residues ARG152, SER179, and SER246 were identified as secondary hot spots for sesamin.

Sesamin inhibited neuraminidase activity similar to oseltamivir. To investigate the effect of sesamin on neuraminidase inhibitory effect, direct ELISA assay of neuraminidase inhibition activity was conducted. The measurement of total sialic acid released from bovine submaxillary mucin substance was taken as the standard curve (Fig. S2). Figure 5 shows that the neuraminidase activity of oseltamivir and sesamin significantly reduced the release of sialic acid from mucin substrate by 0.6- and 0.48-fold, respectively, when compared with the control groups. In order to ensure that neither sesamin nor oseltamivir affected the toxicity levels while inhibiting the neuraminidase activity, measurements of the cell cytotoxicity on PBMCs were taken using the Alamar Blue assay. The results showed that the percentages of cell viability of sesamin and oseltamivir were more than 80% of the control (Fig. S3), indicating that the concentrations 0.5 to 5.0 μg/ml of sesamin and oseltamivir had no toxicity on PBMCs. This data confirmed that sesamin and oseltamivir did not affect the toxicity levels while inhibiting the neuraminidase activity.

Sesamin reduced proinflammatory cytokine and enhanced immunity cytokine production. Next, the effects of sesamin on influenza H1N1-induced PBMCs were investigated using the ELISA method for cytokine release detection and real-time RT-PCR for cytokine gene expressions. Influenza type A H1N1-induced PBMCs were optimized for the release of IL-1β cytokines. It was found that the dilution of influenza type A H1N1 at 1:7,812,500 increased the highest level of IL-1β proteins (Fig. S4). This dilution value of influenza type A H1N1 was selected for further studies concerning the effects of the phytochemicals. The results from the screening studies showed that IL-1β and TNF-α were released into the media in increased amounts by influenza H1N1-induced PBMCs when compared to those of the control groups. When a concentration of sesamin 5.0 μg/ml was cotreated with influenza H1N1-induced PBMCs, the cytokine levels of IL-1β and TNF-α were reduced by 103.6% and 79.7%, respectively (Fig. 6*A*), indicating that sesamin is responsible for the anti-inflammatory activity. Similarly, when a high dosage of oseltamivir (5.0 μg/ml) was used in the treatment, the results

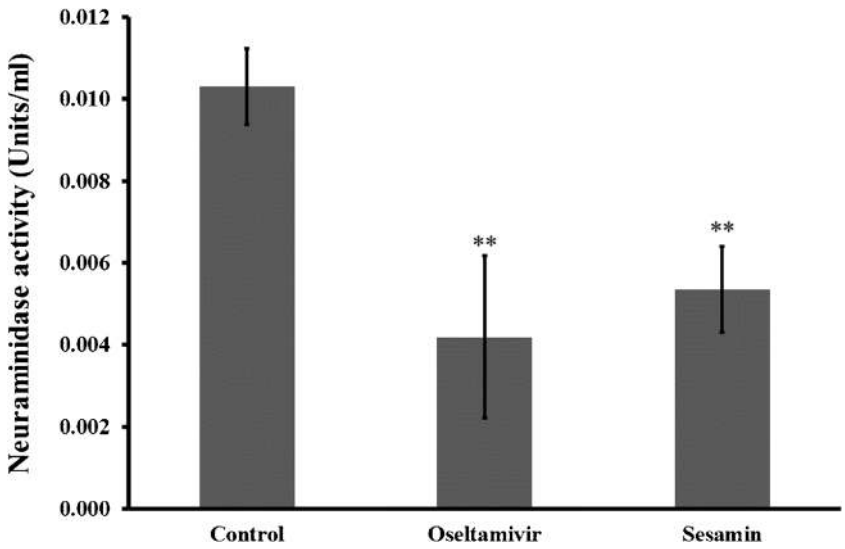

Figure 5. The assay of neuraminidase-inhibition activity (units/ml). Total sialic acid (TSA) released from bovine submaxillary mucin was used in the control group. Data are displayed as mean±SD of three independent experiments. $^{**}p<0.01$, denoted values that were significantly different from the control group.

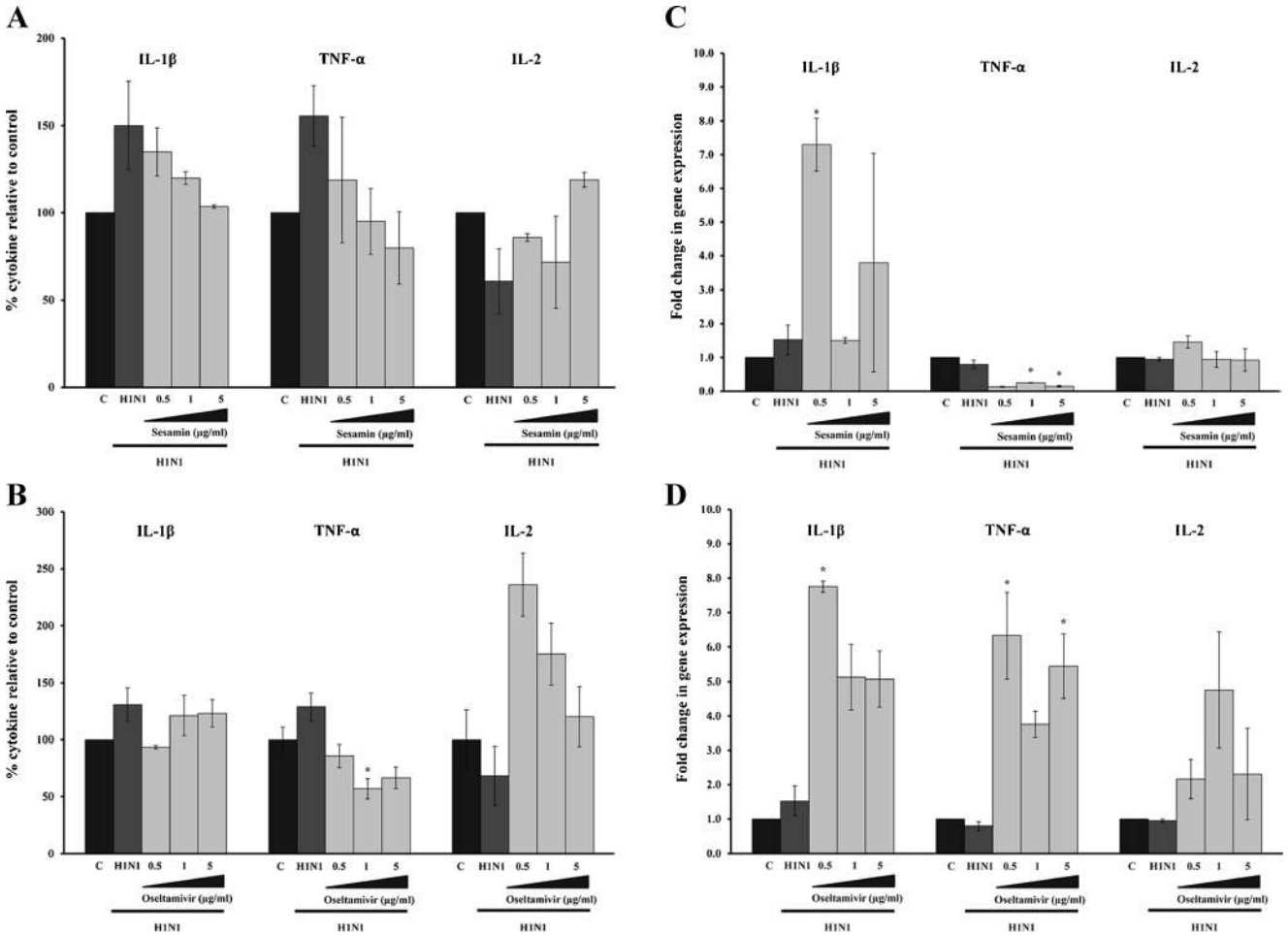

Figure 6. The effects of sesamin (*A*, *C*) and oseltamivir (*B*, *D*) on cytokines both of protein and mRNA levels released from influenza type A H1N1-induced PBMCs. After 24 h of H1N1-induced PBMCs cotreated with sesamin or oseltamivir (Tamiflu®), protein levels of cytokine in the conditional medium were determined using the human IL-1β, TNF-α, and IL-2 Biotrak Easy ELISA, and mRNA levels of cytokine in the cells were determined using real-time RT-PCR. Embryonated chicken eggs were used in the control group. Data are displayed as mean±SE ($n \geq 2$). *$p < 0.05$, denoted values that were significantly different from the H1N1.

showed a surprising level of correspondence with those found under the sesamin treatment: the expression levels of IL-1β and TNF-α were decreased by 123.0% and 66.4%, respectively (Fig. 6*A*). In contrast, the immune responsive cytokine IL-2 numbers reduced influenza H1N1-induced PBMCs by 60.0% when compared with the control groups, whereas a 5.0-μg/ml dosage of sesamin increased the expression levels of IL-2 released in the media by 119.0% (Fig. 6*A*). The expression levels of IL-2 did increase by 235.0% when treated with only 0.5 μg/ml oseltamivir, but higher concentrations always proved to cause a decrease in IL-2 levels in the media (Fig. 6*B*). In contrast, sesamin at low concentration levels seemed to suppress the cytokine storm by reducing the IL-1β levels and increasing the IL-2 levels at the same time.

Moreover, the detection of cytokine gene expressions using real-time RT-PCR showed that H1N1-induced PBMCs increased the IL-1β and TNF-α mRNA levels by 1.56- and 0.80-fold when compared with the control, respectively (Fig. 6*C*, *D*). When cotreatment of sesamin 5.0 μg/ml was done with influenza H1N1-induced PBMCs, the TNF-α mRNA level was reduced by 0.15-fold while the IL-1β mRNA level was induced by 3.80-fold (Fig. 6*C*). As a high dosage of oseltamivir (5.0 μg/ml) was used in the treatment, the results indicated that the mRNA levels of IL-1β and TNF-α were increased 5.07- and 5.45-fold, respectively (Fig. 6*D*). In contrast, the mRNA level of the immune responsive cytokine IL-2 was reduced in influenza H1N1-induced PBMCs 0.95-fold when compared with the control groups, whereas a low dosage (0.5 μg/ml) of sesamin and oseltamivir increased the mRNA levels of IL-2 by 1.45- and 2.16-fold, respectively (Fig. 6*C, D*).

Sesamin inhibits cytokine production though downregulated the phosphorylation of JNK, p38, and ERK1/2 MAPK signaling pathways. The effect of sesamin on the cell signal transduction was evaluated in order to understand the mechanism of sesamin on the reduction of cytokine expression. In this study, we focused on MAPK signaling leading to an

investigation on sesamin inhibiting cytokine production through MAPK signal transduction. Band density analysis of each MAPK signaling molecule was normalized to total form at 1 h treatment showing that H1N1-induced PBMCs increased the phosphorylated form of JNK, p38, and ERK1/2 MAPK signaling transduction by 1.64-, 1.32-, and 3.80-fold when compared with the control, respectively. The cotreatment of a low dose of sesamin (0.5 μg/ml) with H1N1-induced PBMCs had downregulated the phosphorylation of the JNK, p38, and ERK1/2 MAPK signaling cascades by 0.55-, 2.46-, and 1.35-fold when compared with the control, respectively. In addition, the cotreatment of a high dose of sesamin (5 μg/ml) with H1N1-induced PBMCs had downregulated the phosphorylation of JNK, p38, and ERK1/2 MAPK signaling cascades by 0.86-, 0.83-, and 1.30-fold when compared with the control, respectively (Fig. 7).

Discussion

Influenza is still a major cause of morbidity and mortality, and it also causes enormous economic disorder (Ludwig 2009). The mechanism, especially concerning the expression of symptoms and the development of secondary complications that result in respiratory failure, is still not well understood. The excessive inflammation due to cytokine storm and lung failure is still considered an important factor in disease pathogenesis (Schnitzler *et al.* 2009). Despite the success in the development of new antiviral drugs such as oseltamivir in recent years, problems regarding these chemotherapeutic drugs have been reported, such as certain adverse effects, risk of emergence of resistant viruses, and loss of effects due to serotype variation (Hayden *et al.* 1999; Wong *et al.* 2006). Therefore, the development of safe and effective anti-influenza virus drugs remains to be of significant value. Sesamin from the Thai medicinal plant shows high potency in antioxidant properties (Jeng *et al.* 2005), and it has been widely used as a dietary fat-reduction supplement, although no controlled studies on this application have been performed (Utsunomiya *et al.* 2000). Based on this information, we sought the possibility of using sesamin on targeting protein through the use of the computational method by a molecular dynamics simulation and β-propiolactone-inactivated H1N1-induced PBMC model to study its effect on the molecular mechanism.

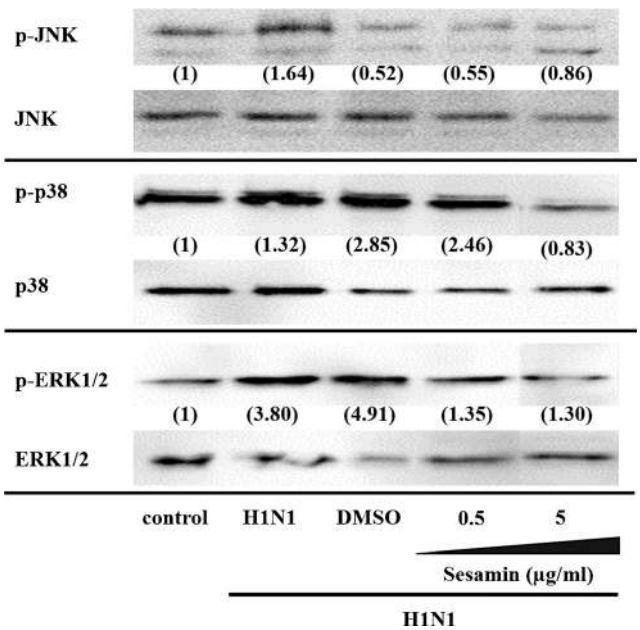

Figure 7. MAPK signaling protein activation in the presence of very concentrated doses of sesamin. After H1N1-induced PBMCs were cotreated with sesamin for 1 h, MAPK signal protein activation in cells was determined using western blotting. The *numbers* denote the quality density value based on Quantity One 4.6.5 software. The data represents three independent studies.

The molecular dynamic simulation showed the new molecular binding structure of sesamin with the 2009 influenza virus type A H1N1 crystallized structure, indicating that sesamin might be used as an alternative antiviral H1N1 compound. Although the neuraminidase inhibitor drugs including oseltamivir and zanamivir also bind the 2009 influenza virus type A H1N1 crystallized structure, these drugs showed an interaction with different amino acids. Furthermore, sesamin inhibits neuraminidase activity similar to oseltamivir. The assay of neuraminidase inhibition activity is based on the measurement of TSA released from bovine submaxillary mucin (Kongtawelert *et al.* 2003), indicating that this assay is not only specific for H1N1 neuraminidase but also detects viruses which expressed neuraminidase. Thus, sesamin can display the specific purpose to bind with the influenza virus type A H1N1 and to inhibit viruses containing neuraminidase activity.

In this study, we used the β-propiolactone-inactivated influenza virus type A H1N1 (Garlick *et al.* 1976; Honda-Okubo *et al.* 2014) antigen-induced PBMC model to study the antiviral activity of sesamin. However, previous studies have recommended using the mouse infection model as the primary tool for studying the anti-influenza virus effects on early immune responses during influenza virus infection (Liu *et al.* 2008). The β-propiolactone-inactivated H1N1 antigen was found to lose RNA-dependent RNA polymerase activity (Garlick *et al.* 1976) but it can induce host cells leading to immunity response (Tamura *et al.* 2005). In addition, we used HAU, which is a traditional protein-based virus quantification assay, for virus quantification and the optimized condition of β-propiolactone-inactivated H1N1-induced PBMCs for further studies concerning the effects of the phytochemicals (Fig. S4). Moreover, phytochemicals, which inhibit the cytokine storm and increase immune response, have never been studied concerning their anti-influenza virus effect on

PBMCs. The PBMC suspension contains about 10% monocytes, which release IL-1β and TNF-α, and 90% lymphocytes which release IL-2 (Brincks *et al.* 2008). Therefore, the influenza type A H1N1-induced PBMC model was useful to investigate the effect of phytochemicals from sesamin on cytokine production.

IL-1β and TNF-α play an important role on stimulating neutrophil and macrophage functions (Veckman *et al.* 2006). In addition, these cytokines stimulated the production of other cytokines such as IL-6 and IL-8 and other chemokines leading to the cytokine storm (Headley *et al.* 1997; Van Reeth 2000). Moreover, macrophages are antigen-presenting cells which stimulate adaptive host defense T cells by presenting influenza A viral peptides, resulting in the production of IL-2 that sends a signal to the white blood cells in propagation for the fight against the virus (Lee *et al.* 2007). H1N1-induced PBMCs upregulated IL-1β and TNF-α levels but downregulated IL-2 both in terms of mRNA and protein levels, suggesting that H1N1-induced PBMCs produced and released cytokines leading to a cytokine storm while suppressing other immune cells. Interestingly, sesamin reversed these effects of H1N1. In addition, oseltamivir also increased IL-1β and TNF-α levels similar to H1N1-induced PBMCs. In contrast, oseltamivir increased IL-2, suggesting that it might be activated by immune cells in inhibiting H1N1-induced PBMCs due to an activation of the immune system. Even though our data did not show significant differences in cytokine production from β-propiolactone-inactivated H1N1-induced PBMCs, the trend of our data showed that sesamin reduced IL-1β and TNF-α levels and increased IL-2 levels. The cytokine concentrations were correlated with cytokine mRNA gene expressions, which showed that sesamin significantly reduced TNF-α levels and increased IL-2 levels. Furthermore, we observed that the effect of sesamin on IL-1β levels and the effect of oseltamivir on IL-1β and TNF-α mRNA levels were not correlated with protein expression levels, and these effects might be caused by the detection time of the mRNA level as we collected the cells at the same time the cytokine was released into the media at 24 h. Therefore, sesamin inhibits influenza type A H1N1 infection via reduced IL-1β and TNF-α levels leading to inhibition of the cytokine storm and increased IL-2 levels leading to a stimulation of immune response.

The mechanism of β-propiolactone-inactivated H1N1 uses the same signaling pathways as H1N1 when infecting host cells (Garlick *et al.* 1976), which involves many signaling cascades that occur through the NF-kB, PI3K/Akt, PKC/PKR, TLR/RIG-I, and MAPK signaling pathways (Gaur *et al.* 2011). In this study, we used embryonic chicken eggs, which were used for the culture of H1N1 virus as a control to compare the effects of inactivated H1N1-induced PBMCs. A previous report has shown that oseltamivir binds to neuraminidase and activates TLR7 signaling molecules in order to inhibit the release of H1N1-induced dendritic cells and macrophages (Chen *et al.* 2012). Our data demonstrated that sesamin inhibited influenza type A virus H1N1 infection via reduced neuraminidase activity. Sesamin reduces inflammatory cytokines (IL-1β and TNF-α) and increases immune responsive cytokine (IL-2) expression via the inhibition of the MAPK (p-JNK, p-p38, and p-ERK1/2) signaling pathways. These observations were consistent with a previous study, which showed that sesamin downregulated p38 and JNK MAPK signaling pathways via IL-1β-induced human articular chondrocytes (Phitak *et al.* 2012). Moreover, a recent report has shown that andrographolide inhibited the H1N1-infected cell model, while using the H1N1-infected respiratory epithelial cells and coculturing with the immunological cells including the dendritic cells, macrophage, and monocytes, via the RIG-I-like receptor signaling pathway (Yu *et al.* 2014). Thus, it may be that sesamin can inhibit H1N1-induced PBMCs not only though MAPK inhibition but also via other signaling cascades, which should be further investigated.

Our results demonstrated that the antiviral effect of sesamin might be related to the inhibition of neuraminidase activity and the reduction of inflammatory cytokines via the MAPK signaling pathway. Therefore, sesamin could be applied as an alternative antiviral treatment; however, the side effects that occur besides the desired therapeutic effect need to be considered. The intention of this study is to design a model that will be useful in the efforts made toward producing new inhibitors that are able to bind to the proposed critical sites.

Conclusions

This study revealed important results that highlight the novel strategies used in the early phases of preclinical development of sesamin from a Thai medicinal plant for the prevention of viral induction of the cytokine storm. The molecular docking studies of sesamin show that it could be bound to the binding region of the 2009 influenza virus type A H1N1. However, there are some stability configuration issues, as observed in the structural changes during MD simulations. Furthermore, the results showed that sesamin reduced the release of IL-1β and TNF-α leading to an inhibition of the cytokine storm and enhancing the activity of the immune cells via an increase of IL-2 levels through the downregulation of the phosphorylation of JNK, p38, and ERK1/2 MAPK signaling pathways. Therefore, this study found sesamin to be of great interest and worthy of further study as a potential new pharmacological agent in the prevention and treatment of immune-induced inflammatory disorders.

Acknowledgments Gratitude is extended to the Royal Golden Jubilee Ph.D. Program Grants (PHD/0087/2553 to K.F.) and the Graduate School of Chiang Mai University (K.F.). The authors would like to gratefully acknowledge Prof. Yong Poovorawan, Faculty of Medicine,

Chulalongkorn University, Bangkok, Thailand, for providing β-propiolactone-inactivated influenza virus type A H1N1; Thailand Excellence Center for Tissue Engineering and Stem Cells, Department of Biochemistry, Faculty of Medicine, Chiang Mai University, Chiang Mai, Thailand, and the Computational Simulation and Modeling Laboratory (CSML), Department of Chemistry, Faculty of Science, Chiang Mai University for the computer access; and the Computational Nanoscience Consortium (CNC), the National Nanotechnology Center (NANOTEC), Thailand, for access to Discovery Studio Modeling, version 2.5 program packages.

References

Boeuf P, Vigan-Womas I, Jublot D, Loizon S, Barale JC, Akanmori BD, Mercereau-Puijalon O, Behr C (2005) CyProQuant-PCR: a real time RT-PCR technique for profiling human cytokines, based on external RNA standards, readily automatable for clinical use. BMC Immunol 6:5

Brincks EL, Kucaba TA, Legge KL, Griffith TS (2008) Influenza-induced expression of functional tumor necrosis factor-related apoptosis-inducing ligand on human peripheral blood mononuclear cells. Hum Immunol 69:634–646

Büchen-Osmond C (2006) International Committee on Taxonomy of Viruses. Index of viruses—orthomyxovirus. Columbia University, New York, the universal virus database, version 4

Case DA, Cheatham TE 3rd, Darden T, Gohlke H, Luo R, Merz KM Jr, Onufriev A, Simmerling C, Wang B, Woods RJ (2005) The Amber biomolecular simulation programs. J Comput Chem 26:1668–1688

Chambers TM, Hinshaw VS, Kawaoka Y, Easterday BC, Webster RG (1991) Influenza viral infection of swine in the United States 1988–1989. Arch Virol 116:261–265

Chen C, Jiang ZY, Yu B, Wu XL, Dai CQ, Zhao CL, Ju DH, Chen XY (2012) Study on the anti-H1N1 virus effects of quercetin and oseltamivir and their mechanism related to TLR7 pathway. J Asian Nat Prod Res 14:877–885

Chong LT, Duan Y, Wang L, Massova I, Kollman PA (1999) Molecular dynamics and free-energy calculations applied to affinity maturation in antibody 48G7. Proc Natl Acad Sci U S A 96:14330–14335

Colman PM (1994) Influenza virus neuraminidase: structure, antibodies, and inhibitors. Protein Sci: Publ Protein Soc 3:1687–1696

Committee WHOE (1980) A revision of the system of nomenclature for influenza viruses: a WHO memorandum. Bull WHO 58:585–591

Cowan MM (1999) Plant products as antimicrobial agents. Clin Microbiol Rev 12:564–582

Dai X, Zhang L, Hong T (2011) Host cellular signaling induced by influenza virus. Sci China Life Sci 54:68–74

Darden TA, Pedersen LG (1993) Molecular modeling: an experimental tool. Environ Health Perspect 101:410–412

Dawood FS, Jain S, Finelli L, Shaw MW, Lindstrom S, Garten RJ, Gubareva LV, Xu X, Bridges CB, Uyeki TM (2009) Emergence of a novel swine-origin influenza A (H1N1) virus in humans. N Engl J Med 360:2605–2615

Donini OA, Kollman PA (2000) Calculation and prediction of binding free energies for the matrix metalloproteinases. J Med Chem 43: 4180–4188

Garlick B, Avery RJ (1976) Inactivation of Newcastle disease virus by beta-propiolactone. Arch Virol 52:175–179

Gaur P, Munjhal A, Lal SK (2011) Influenza virus and cell signaling pathways. Med Sci Monit : Int Med J Exp Clin Res 17:RA148–154

Gohlke H, Kiel C, Case DA (2003) Insights into protein-protein binding by binding free energy calculation and free energy decomposition for the Ras-Raf and Ras-RalGDS complexes. J Mol Biol 330:891–913

Hayden FG, Atmar RL, Schilling M, Johnson C, Poretz D, Paar D, Huson L, Ward P, Mills RG (1999) Use of the selective oral neuraminidase inhibitor oseltamivir to prevent influenza. N Engl J Med 341:1336–1343

Headley AS, Tolley E, Meduri GU (1997) Infections and the inflammatory response in acute respiratory distress syndrome. Chest 111: 1306–1321

Honda-Okubo Y, Kolpe A, Li L, Petrovsky N (2014) A single immunization with inactivated H1N1 influenza vaccine formulated with delta inulin adjuvant (Advax) overcomes pregnancy-associated immune suppression and enhances passive neonatal protection. Vaccine 32:4651–4659

Hou T, Zhang W, Case DA, Wang W (2008) Characterization of domain-peptide interaction interface: a case study on the amphiphysin-1 SH3 domain. J Mol Biol 376:1201–1214

Jeng KC, Hou RC, Wang JC, Ping LI (2005) Sesamin inhibits lipopolysaccharide-induced cytokine production by suppression of p38 mitogen-activated protein kinase and nuclear factor-kappaB. Immunol Lett 97:101–106

Kongtawelert P, Tangkijvanich P, Ong-Chai S, Poovorawan Y (2003) Role of serum total sialic acid in differentiating cholangiocarcinoma from hepatocellular carcinoma. World J Gastroenterol: WJG 9: 2178–2181

Lee DCW, Lau ASY (2007) Avian influenza virus signaling: implications for the disease severity of H5N1 infection. Signal Transduct 7:64–80

Liu AL, Liu B, Qin HL, Lee SM, Wang YT, Du GH (2008) Anti-influenza virus activities of flavonoids from the medicinal plant Elsholtzia rugulosa. Planta Med 74:847–851

Livak KJ, Schmittgen TD (2001) Analysis of relative gene expression data using real-time quantitative PCR and the 2(−Delta Delta C(T)) method. Methods 25:402–408

Ludwig S (2009) Targeting cell signalling pathways to fight the flu: towards a paradigm change in anti-influenza therapy. J Antimicrob Chemother 64:1–4

Mogensen TH, Paludan SR (2001) Molecular pathways in virus-induced cytokine production. Microbiol Mole Biol Rev: MMBR 65:131–150

Palese P, Shaw ML (2007) Orthomyxoviridae: the viruses and their replication. In: Knipe DM, Howley PM (eds) Fields virology, 5th edn. Lippincott, Williams and Wilkins, Philadelphia, p 1647–1690

Phitak T, Pothacharoen P, Settakorn J, Poompimol W, Caterson B, Kongtawelert P (2012) Chondroprotective and anti-inflammatory effects of sesamin. Phytochemistry 80:77–88

Provenzano M, Mocellin S, Bonginelli P, Nagorsen D, Kwon SW, Stroncek D (2003) Ex vivo screening for immunodominant viral epitopes by quantitative real time polymerase chain reaction (qRT-PCR). J Transl Med 1:12

Russell RJ, Haire LF, Stevens DJ, Collins PJ, Lin YP, Blackburn GM, Hay AJ, Gamblin SJ, Skehel JJ (2006) The structure of H5N1 avian influenza neuraminidase suggests new opportunities for drug design. Nature 443:45–49

Sali A, Blundell TL (1993) Comparative protein modelling by satisfaction of spatial restraints. J Mol Biol 234:779–815

Schnitzler SU, Schnitzler P (2009) An update on swine-origin influenza virus A/H1N1: a review. Virus Genes 39:279–292

Tamura S, Tanimoto T, Kurata T (2005) Mechanisms of broad cross-protection provided by influenza virus infection and their application to vaccines. Jpn J Infect Dis 58:195–207

Utsunomiya T, Chavali SR, Zhong WW, Forse RA (2000) Effects of sesamin-supplemented dietary fat emulsions on the ex vivo production of lipopolysaccharide-induced prostanoids and tumor necrosis factor alpha in rats. Am J Clin Nutrit 72:804–808

Van Reeth K (2000) Cytokines in the pathogenesis of influenza. Vet Microbiol 74:109–116

Vavricka CJ, Li Q, Wu Y, Qi J, Wang M, Liu Y, Gao F, Liu J, Feng E, He J, Wang J, Liu H, Jiang H, Gao GF (2011) Structural and functional

analysis of laninamivir and its octanoate prodrug reveals group specific mechanisms for influenza NA inhibition. PLoS Pathog 7: e1002249

Veckman V, Osterlund P, Fagerlund R, Melen K, Matikainen S, Julkunen I (2006) TNF-alpha and IFN-alpha enhance influenza-A-virus-induced chemokine gene expression in human A549 lung epithelial cells. Virology 345:96–104

Wallace AC, Laskowski RA, Thornton JM (1995) LIGPLOT: a program to generate schematic diagrams of protein-ligand interactions. Protein Eng 8:127–134

Wang MJ, Lin WW, Chen HL, Chang YH, Ou HC, Kuo JS, Hong JS, Jeng KC (2002) Silymarin protects dopaminergic neurons against lipopolysaccharide-induced neurotoxicity by inhibiting microglia activation. Eur J Neurosci 16:2103–2112

Weber W, Hünenberger PH, McCammon JA (2000) Molecular dynamics simulations of a polyalanine octapeptide under Ewald boundary conditions: influence of artificial periodicity on peptide conformation. J Phys Chem B 104:3668–3675

Wong SS, Yuen KY (2006) Avian influenza virus infections in humans. Chest 129:156–168

Wu G, Robertson DH, Brooks CL 3rd, Vieth M (2003) Detailed analysis of grid-based molecular docking: a case study of CDOCKER-A CHARMm-based MD docking algorithm. J Comput Chem 24: 1549–1562

Yu B, Dai CQ, Jiang ZY, Li EQ, Chen C, Wu XL, Chen J, Liu Q, Zhao CL, He JX, Ju DH, Chen XY (2014) Andrographolide as an anti-H1N1 drug and the mechanism related to retinoic acid-inducible gene-I-like receptors signaling pathway. Chin J Integr Med 20: 540–545